Proceedings of Meetings on Acoustics

Volume 9, 2010 http://asa.aip.org

159th Meeting
Acoustical Society of America/NOISE-CON 2010
Baltimore, Maryland
19 - 23 April 2010
Session 4aSA: Structural Acoustics and Vibration

4aSA9. Development of a Pseudo-uniform Structural Quantity for Use in Active Structural Acoustic Control

Jeff Fisher*, Daniel A. Manwill, Jonathan D. Blotter, Kent L. Gee and Scott D. Sommerfeldt

***Corresponding author's address: Mechanical Engineering, Brigham Young University, Brigham Young University, Provo, UT 84602, jeffery.m.fisher@gmail.com**

Active structural acoustic control has been an area of increasing interest over the past decade with an increase in the search for a suitable error quantity. Current errors require the use of large amounts of accelerometers distributed across the entire structure to provide a suitable estimate of the volume velocity, as research has shown this quantity to be highly related to the overall acoustic radiation. Other methods involve a previous knowledge of the number of contributing acoustic radiation modes as well as an array of accelerometers to extract these modes. The purpose of this paper is to investigate a new structural quantity which when used in an active control situation attenuates the acoustic radiation over a large range of frequencies. The benefits of this technique are that it involves only a single point measurement and the placement of this sensor on the structure is fairly arbitrary. The results given are based on a simply supported plate and are purely analytical.

Published by the Acoustical Society of America through the American Institute of Physics

 [DOI: 10.1121/1.3486521]
Received 5 Aug 2010; published 17 Aug 2010
Proceedings of Meetings on Acoustics, Vol. 9, 065005 (2010)

INTRODUCTION

The original abstract and title have been altered due to the lack of general and practical use in dealing with structural energy density and structural power flow in an active structural acoustic control situation. The original work was entitled Relationships between structural energy density, power flow and their influence on acoustic intensity.

Active Structural Acoustic Control (ASAC) which involves altering the vibrations of a structure to obtain a vibration field which acoustically radiates less efficiently than an uncontrolled case resulting in less acoustic radiation from the given structure is an ongoing area of research.

Certain energy based structural metrics and their influence on acoustic radiation have been investigated. A well known quantity which has been investigated is structural intensity, or structural power flow. However, it has been shown that structural power flow has little effect on acoustic intensity[1] and thus shows little promise as a control metric. Structural energy density has also been looked at and could be used as a control metric but lacks spatial uniformity, thereby requiring specific placement locations on the structure in order to produce desired results[2]. The control of acoustic radiation modes has shown promise but requires the use of multiple sensors and knowledge of the radiation modes which contribute significantly to the overall radiation[3,4].

Research has suggested that most of the acoustic radiation from a structure is attributed to the more global quantity of volume velocity[5,6]. This can be viewed from Rayleigh's integral given as:

$$P(r,t) = \frac{j\omega\rho}{2\pi} e^{j\omega t} \int_S \frac{\tilde{v}_n(r_s) e^{-jkR}}{R} dS \tag{1}$$

where **r** is the position vector of the observation point, $\mathbf{r_s}$ is the position on the surface having a velocity amplitude $\tilde{v}_n$ and R is the magnitude of r-r_s. As can be seen, reduction in the overall level of $\tilde{v}_n$ on the structure will decrease the pressure at all points in the field. For this reason, a spatially uniform quantity that is related to volume velocity should provide a good structural quantity for minimization, which would only require the use of a single point sensor. A quantity that represents the complete velocity state and combines the bending and twisting velocities in the structure has been developed. This quantity has been termed V_{comp} for complete velocity field. The derivation and use of this term are discussed the following sections.

DERIVATION OF V_{COMP}

V_{comp} is a quantity which was developed to represent the complete velocity state in the structure. This quantity is then used as the minimization quantity in an active control system. For the derivation of V_{comp}, an analytical model of a simply supported, damped, plate with multiple point force locations was used. The displacement of the plate is given by Eqs 2-5.

$$w(x,y) = \sum_{q=1}^{F} \frac{f_q}{\rho_s h} \sum_{m}^{\infty} \sum_{n}^{\infty} \frac{W_{mn}(x,y) W_{mn}(x_q,y_q)[\omega_{mn}^2 - \omega^2 - i\eta\omega_{mn}^2]}{[\omega_{mn}^2 - \omega^2]^2 + \eta^2\omega_{mn}^4} \tag{2}$$

$$W_{mn}(x,y) = \frac{2}{\sqrt{L_x L_y}} sin\left(\frac{m\pi x}{L_x}\right) sin\left(\frac{n\pi y}{L_y}\right) \tag{3}$$

$$\omega_{mn} = \sqrt{\frac{D}{\rho_s h}\left(\frac{m^2\pi^2}{L_x^2} + \frac{n^2\pi^2}{L_y^2}\right)} \tag{4}$$

$$D = \frac{Eh^3}{12(1-\nu^2)} \tag{5}$$

where f_q is the amplitude of the driving force, $\rho_s$is the density of the material, E is Young's modulus, ν is Poisson's ratio, h is the plate thickness, and L_x and $L_y$are the plate dimensions. The structural damping ratio is given by η, ω is the driving frequency in radians, and m and n are structural mode shape numbers. A steel plate of dimensions 0.438 m x 0.762 m x 0.001 m with a structural damping ratio of 0.001 was used. The first fifteen structural modes of the plate as computed by Eq. 4 are given in Table 1.

Table 1: Analytically computed modal frequencies and corresponding mode shapes of a simply supported plate

Mode	Modal frequency Hz
(1,1)	13.390
(2,1)	24.889
(1,2)	42.059
(3,1)	44.055
(2,2)	53.559
(4,1)	70.888
(3,2)	72.725
(1,3)	89.841
(4,2)	99.557
(2,3)	101.341
(5,1)	105.386
(3,3)	120.507
(5,2)	134.056
(4,3)	147.339
(6,1)	147.552

For the (1,1) mode of the plate excited by a single point force at an anti-node, four velocity terms were computed. These are the transverse, rocking and twisting velocities, given by

$$\left(\frac{dw}{dt}\right)^2, \left(\frac{d^2w}{dxdt}\right)^2, \left(\frac{d^2w}{dydt}\right)^2, \left(\frac{d^3w}{dxdydt}\right)^2 \tag{6}$$

and are plotted in Figure 1.

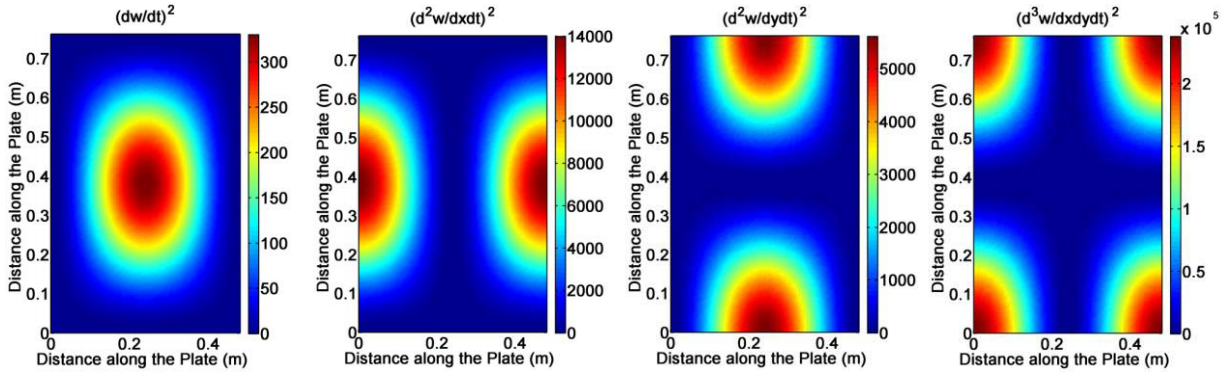

Figure 1. Four terms used in V_{comp}

Looking at these four velocity terms, it can be seen that each of the four terms covers a different spatial portion of the plate and with a combination of these terms, a fairly uniform velocity field can be developed. In order to combine these four terms, a simple linear combination was performed as given by Eq. 7.

$$V_{comp} = \alpha\left(\frac{dw}{dt}\right)^2 + \beta\left(\frac{d^2w}{dxdt}\right)^2 + \gamma\left(\frac{d^2w}{dydt}\right)^2 + \delta\left(\frac{d^3w}{dxdydt}\right)^2 \quad (7)$$

Using a simple gradient based algorithm and the standard deviation of V_{comp} at each of the calculated points on the plate as the cost function, along with a constraint that the sum of α,β,γ,δ must be equal to two, the values for α,β,γ,δ are given in Table 2. If the sum of α,β,γ,δ were not given a constraint, the values of all four terms would be driven to zero. The value of two was chosen arbitrarily, as the importance lies in the ratios of the four terms.

Table 2: α,β,γ,δ for the (1,1) structural mode

α	β	γ	δ
1.8453	0.0435	0.1086	0.0026

Using theses scaling values, the analytically computed V_{comp} for the (1,1) structural mode is shown in Figure 2. The color scale verifies that the V_{comp} computation for this mode using the coefficients of Table 2 is very uniform over the entire plate.

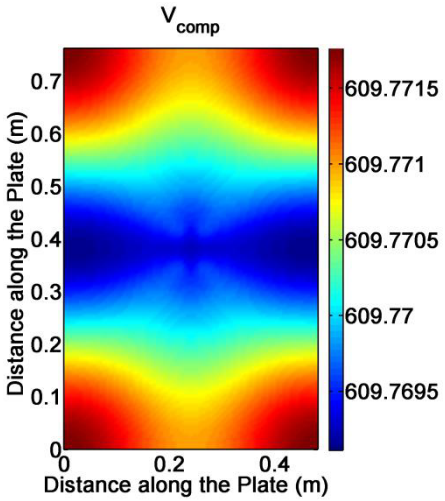

Figure 2. V_{comp} at the (1,1) structural mode

The scaling factors shown for the (1,1) mode in Table 2 do vary based on the structural mode but this variance is comparatively small and does not largely affect the overall outcome. An average of the scaling factors based on the first fifteen structural modes will be used and is given in Table 3.

Table 3: Average scaling factors from the first 15 structural modes

α	β	γ	δ
1.9456	0.0216	0.0325	3.497e-5

Because the spatial derivatives of this quantity are only first and second order, a simple measurement array using four transducers mounted in a rectangular pattern will be required as shown Figure 3.

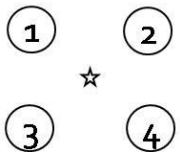

Figure 3. V_{comp} sensor configuration

ASAC ANALYTICAL VERIFICATIONS

Radiated Power

To view the effect of controlling V_{comp} on the simply supported plate, the power radiated from the plate was chosen as the benchmark and was calculated using the well known elementary radiator method[6,7]. This method involves breaking the structure into a spatial grid of small acoustic radiators as shown in Figure 4. This particular method was selected because of the ease of calculating the acoustic radiation modes as well.

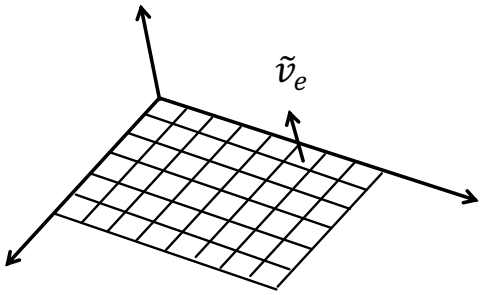

Figure 4. Panel broken up into elementary radiators

The power radiated from a plate using elementary radiators is given by Eq. 8.

$$\bar{P}(\omega) = \{\tilde{v}_e\}^H [R] \{\tilde{v}_e\} \tag{8}$$

where $\{\tilde{v}_e\}$ is a velocity vector containing the velocities of the individual elements and

$$[R] = \frac{\omega^2 \rho_0 A_e^2}{4\pi c} \begin{bmatrix} 1 & \frac{\sin(kR_{12})}{kR_{12}} & \dots & \frac{\sin(kR_{1R})}{kR_{1R}} \\ \frac{\sin(kR_{21})}{kR_{21}} & 1 & \dots & \dots \\ \dots & \dots & \ddots & \dots \\ \frac{\sin(kR_{R1})}{kR_{R1}} & \dots & \dots & 1 \end{bmatrix} \tag{9}$$

where R_{mn} is the distance between the mth and nth elements.

The control of V_{comp} was performed by selecting a primary disturbance location, a control force location and an error sensor location. An optimization routine was used to determine the correct phase and magnitude of the control force to effectively minimize the cost function (V_{comp}) at the error sensor location. Figure 5 shows the disturbance location, control location and seven error sensor locations. The error sensors were used independently to determine if large differences occurred in the radiated power due to error sensor locations.

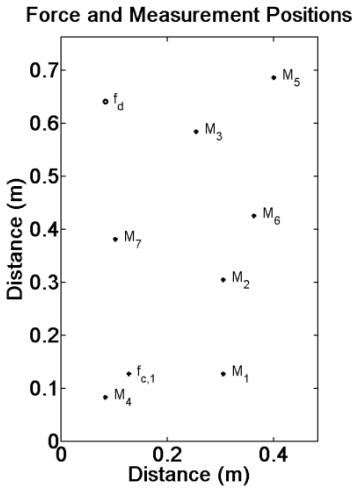

Figure 5: Force and Measurement Locations

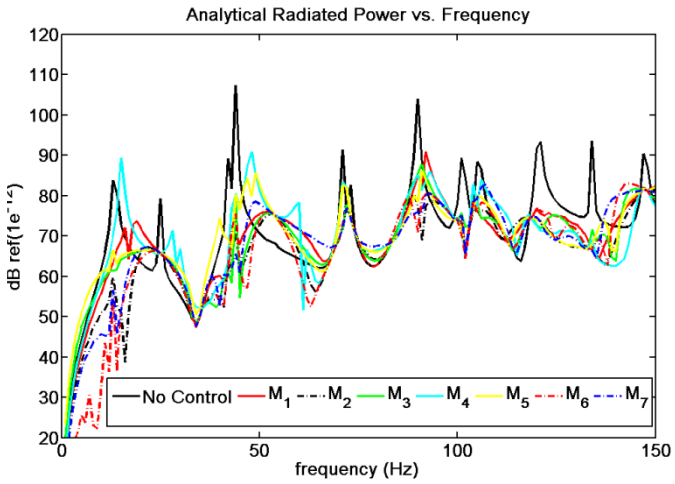

Figure 6: Radiated Power with control at multiple locations

Based on minimizing V_{comp} at these error sensor locations, the radiated power before and after control is shown in Figure 6. The radiated power at frequencies spanning the first fifteen structural modes can be seen in Figure 6. Locations M_1, M_2, M_3, M_6, M_7 produced good results while locations M_4 and M_5 produced an overall undesirable effect leading to the notion that control is fairly independent of sensor location with the exception that error sensors should not be placed near the corners of the plate. For the remainder of this paper, location M_2 will be isolated in order to gain a better understanding of the benefits of V_{comp} control. The radiated power based on V_{comp} control at location M_2 is shown in Figure 7

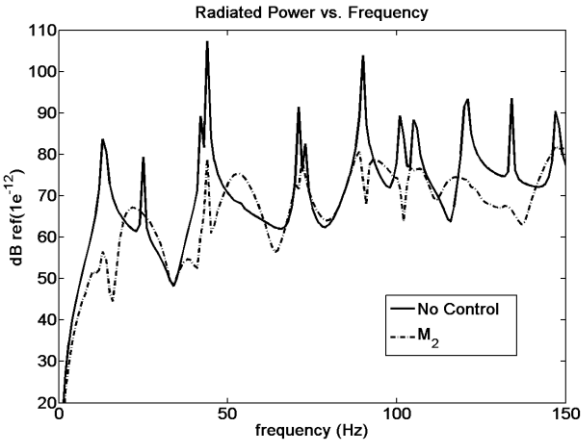

Figure 7. Radiated Power Before and After Control at location M_2

As can be viewed in the results, controlling the quantity V_{comp} nearly always decreased the radiated power and overall produced a significant reduction. At some frequencies the radiated power was boosted but most frequencies saw a large reduction in radiated power and each of the resonance peaks was attenuated significantly. The largest benefit of controlling V_{comp} is that the control performance is largely independent of sensor location. To validate this, the sensor was moved to multiple locations on the plate and the experiment repeated with comparable results at most all locations. It should be noted that when the sensor was placed in the corners, V_{comp} performed poorly. However, when placed in locations further from the corners of the plate, the control of V_{comp} attenuated almost all of the peaks significantly and even provided control at frequencies other than the resonance frequencies. This result allows the sensor to be placed at a relatively arbitrary location and the placement required no previous knowledge of

the vibrating structure which adds an immense benefit to this technique. With V_{comp} at the M_2 location, the overall attenuation with a frequency span incorporating the first fifteen structural modes was 4.5 dB.

Acoustic Radiation Modes

A reason for the overall success of V_{comp} can be identified when looking at acoustic radiation modes. In the past, controlling radiation modes has been an effective way to control the power radiated from a panel. However, the structural geometry associated with the vibrations must be known prior to this because sensors need to be placed in locations conducive to sensing all significant radiation modes present. In most cases, structural vibrations cannot be known without equipment such as multiple accelerometer arrays or an SLDV, and the radiation modes cannot be obtained without some numerical analysis of the structure. Furthermore, if many modes are present, these techniques require the use of a large number of sensors. Referring to the quantities used in V_{comp} and the first four acoustic radiation modes, a relationship exists between the two. The first radiation mode can be looked at like a transverse velocity, the second a rocking in x, the third a rocking in y, and the fourth, a twisting term. Given the [R] matrix as solved for above, the acoustic radiation modes are given by:

$$[R] = [Q]^T[\Lambda][Q] \tag{10}$$

where [Q] is a matrix of orthogonal eigenvectors and [Λ] is a diagonal matrix of eigenvalues. The relative magnitudes of the radiation modes are given by the elements of [Λ], and the shape is given by the corresponding row of [Q]. The shapes of the first six acoustic radiation modes are shown in Figure 8.

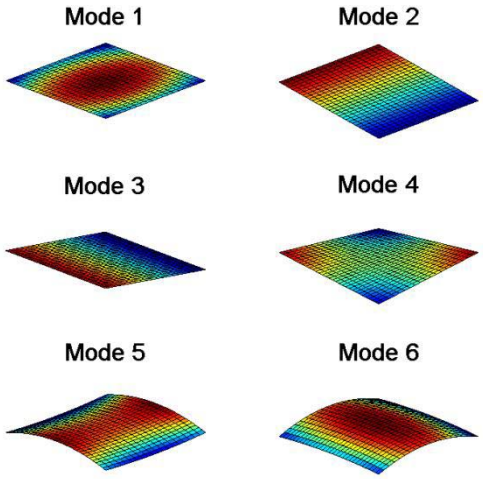

Figure 8. Radiation modes shapes

Using radiation modes, the overall power radiated is given by

$$\bar{P}(\omega) = \{\tilde{y}\}^H[\Lambda]\{\tilde{y}\} = \sum_{r=1}^{R} \lambda_r |\tilde{y}_r|^2 \tag{11}$$

$$\{\tilde{y}\} = [Q]\{\tilde{v}_e\} \tag{12}$$

where R is the total number of elements and λ_r, $\tilde{y}_r$ are the components corresponding to the element of interest. The shape of the radiation mode is dependent on frequency. The higher the frequency, the higher the curvature there is in the individual radiation modes. The power radiated by the individual acoustic radiation modes is given by

$$\bar{P}_m(\omega) = \lambda_m |\tilde{y}_m|^2 \tag{13}$$

with *m* being the individual mode. The control of the first six radiation modes was analyzed to see the effects. The individual power radiated from the modes was calculated using Equation (13). A comparison of the individual modes before and after control of V_{comp} is given in Figure 9.

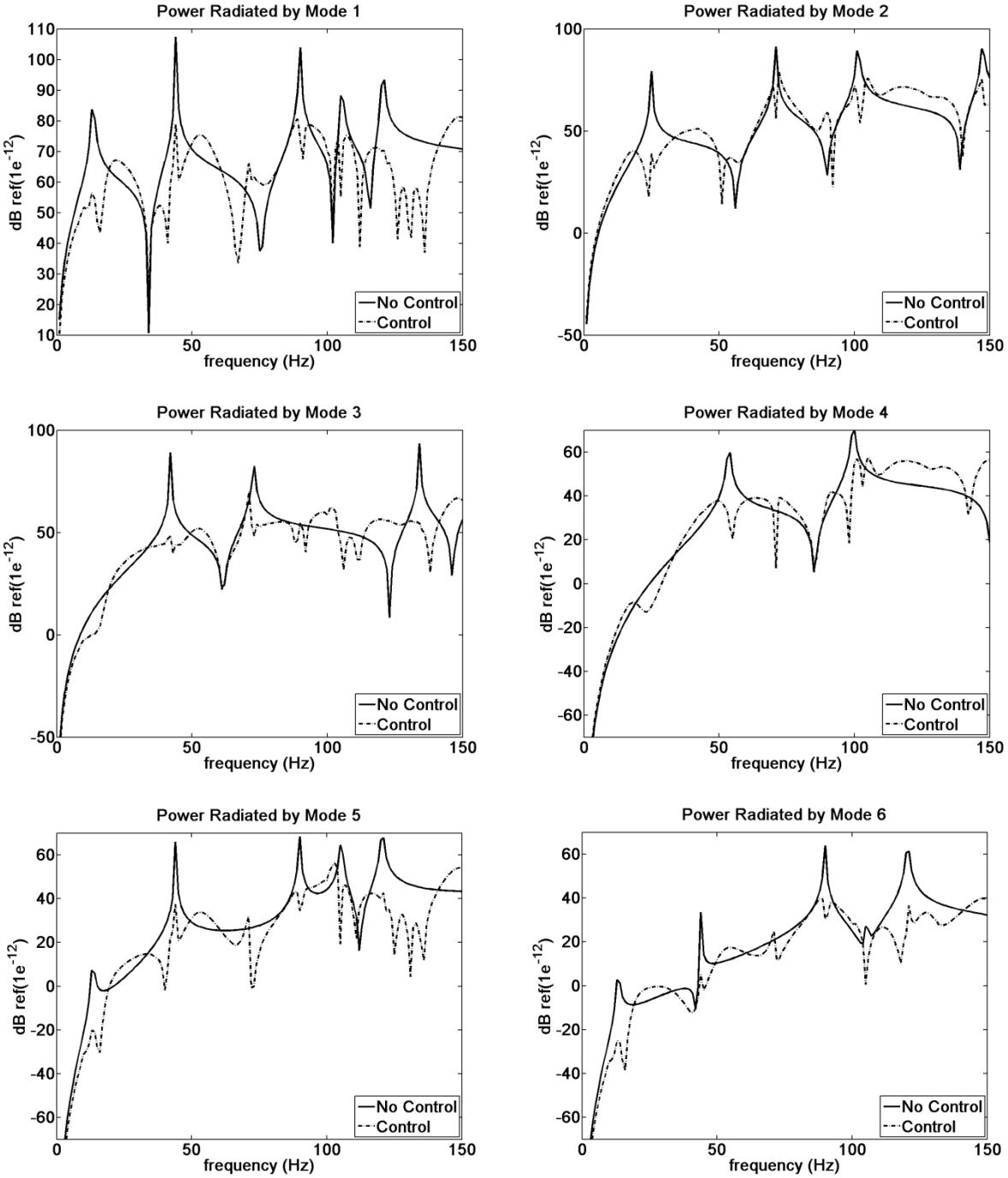

Figure 9. Power radiated by individual radiation modes

Using V_{comp}, most all of the peaks of the individual radiation modes were significantly reduced. In many of the acoustic radiation mode plots, the peak corresponding to the (2,2) mode saw a boost in power. This results because originally the (2,2) mode is a very inefficient radiating mode, but when modified during the control of V_{comp} restructures into a more efficiently radiating structure.

BENEFITS AND CONCLUSIONS

The new structural quantity, V_{comp}, produces desirable results in the active control of structures. The benefits include: control at higher structural modes, control largely independent of sensor location, and need for only a single point measurement of V_{comp} with a compact sensor. The control at higher frequencies can be explained by the control of multiple acoustic radiation modes, not just a single one. While all of the desirable characteristics are benefits, the most highly sought after is that of the control being largely independent of sensor location. Strictly speaking, this results in a lack of need to know the structural vibrations before placing the sensor. The overall broadband result of V_{comp} control is promising in the area of active control of structural acoustics because of the attenuation achieved, lack of dependency on sensor location, and the number of required measurement transducers. Some of the challenges which need to be investigated further are the importance of the control location, error introduced due to sensor rotation as well as the experimental verification of this control technique.

ACKNOWLEDGMENTS

This work was supported by NSF Grant number CMMI-0826554.

REFERENCES

1. Tanaka, N., Snyder, S. D., Kikushima, Y., & Kuroda, M. (1994). Vortex structural power flow in a thin plate and the influence on the acoustic field. *JASA* , 1563-1574.
2. Daniel Manwill et. al. (2010), On the Use of Energy Based Metrics in Active Structural Acoustic Control. POMA.
3. Snyder, S. D., Brugan, N. C., & Tanaka, N. (2002). An acoustic based modal filtering approach to sensing system design for active control of structural acoustic radiation: Theoretical development. *Mechanical Systems and Signal Processing* , 123-139.
4. Johnson, M. E., & Elliott, S. J. (1995). Active control of sound radiation using volume velocity cancellation. *JASA* , 2174-2186.
5. Sors, T. C., & Elliott, S. J. (202). Volume velocity estimation with accelerometer arrays for active structural acoustic control. *Journal of Sound and Vibration* , 867-883.
6. Elliott, S. J., & Johnson, M. E. (1993). Radiation modes and the active control of sound power. *JASA* , 2194-2204.
7. Fahy, F., & Gardonio, P. (2007). *Sound and Structural Vibration: Radiation, Transmission and Response.* Oxford: Elsevier.